since 1961

Baltica

BALTICA Volume 29 Number 1 June 2016: 3–18
doi: 10.5200/baltica.2016.29.02

Operational algae bloom detection in the Baltic Sea using GIS and AVHRR data

Marcin Kulawiak

Kulawiak, M., 2016. Operational algae bloom detection in the Baltic Sea using GIS and AVHRR data. *Baltica, 29 (1), 3-18.* Vilnius. ISSN 0067-3064.

Manuscript submitted 5 January 2016 / Accepted 14 May 2016 / Published online 14 June 2016

Abstract During the blooming season, algal colonies can, in extreme cases, cover up to 200 000 square kilometres of the Baltic Sea water surface. Because the position and shape of the blooms may significantly change in a very short time due to the influence of wind and waves, regular monitoring of the blooms' development is necessary. Currently, the desired monitoring frequency may only be achieved by means of remote sensing. The article presents a novel method of AVHRR data processing for the purpose of detection of algal blooms in the Baltic Sea. Instead of analysing the value of spectral reflectance of the algae, the algorithm analyses the frequency distribution of normalized difference in reflectance between the visible and near-infrared spectral bands. The proposed method has been implemented and tested as part of an operational Geographic Information System.

Keywords *• GIS • algae • AVHRR • remote sensing • geovisual analytics*

✉ *Marcin Kulawiak (marcin.kulawiak@eti.pg.gda.pl), Gdansk University of Technology, Faculty of Electronics, Telecommunication and Informatics, Department of Geoinformatics, Gabriela Narutowicza street 11/12, 80-233 Gdansk, Poland*

INTRODUCTION

For many years the Baltic Sea has been home to large blooms of microalgae capable of performing photosythesis through the use of pigment chlorophyll and absorption of yellow-orange light (Lignell,1993). They commonly bloom in large colonies, which tend to form large mats on water surface. Given enough nutrition, they easily dominate the reservoir's natural phytoplankton and grow in numbers large enough to make the water dangerous to animals and humans alike (Stewart *et al*. 2006). The presence of microalgae has many adverse effects on the affected basin. First of all, large colonies of microalgae increase water turbidity, which makes it unusable for agricultural and industrial applications (Klapper 1991). Dense colonies of harmful microalgae may also cause problems for sailors and thus negatively affect the local industry (Pitois *et al.* 2000). Aside from affecting water clarity, harmful microalgae tend to generate unpleasant odour which drives away enthusiasts of boating and swimming (Dodds *et al.* 2009). More serious effects of algal blooms include elevation of water pH and oxygen depletion, which have a devastating effect on indigenous flora and fauna of the water reservoir (Havens 2007). Finally, certain types of microalgae, such as cyanobacteria, are highly toxic. For example, ingesting even relatively small amounts of *Microcystis aeruginosa* can damage the subject's liver, intestines, and nervous system (Falconer *et al.* 1983). All of this makes microalgae dangerous to the well-being of humans and animals which are in any way dependant on the affected water reservoir. Although algal blooms are a natural phenomenon, the increase in industrial processes during the 20th century have transformed the ecosystems of certain water reservoirs in such a way that these microorganisms have become a serious threat (Gilbert *et al.* 2005). The Baltic Sea has attracted several types of these organisms, in particular the hepatotoxic *Nodularia spumigena* and *Aphanizomenon flos-aquae*, which tend to form surface accumulations covering a substantial portion of the basin (Sivonen *et al.* 1989).

Monitoring water reservoirs for signs of algal blooms has been a subject of intense research for many years. Aside from in-situ measurements, which are the most reliable but also the most expensive method of microalgae detection, much attention has been paid to development of appropriate remote sensing methods.

Because microalgae tend to form large swaths which may reach ~200 000 km^2 (Kahru, Elmgren 2014), the dense accumulations may be identified visually by analysis of the visible bands. In 1997 Kahru manually prepared a time series of Advanced Very High Resolution Radiometer (AVHRR) images to demonstrate a method of detecting algal blooms in the Baltic Sea by thresholding the swath reflectance in the visible band (Kahru 1997). The method generally worked for large accumulations, but the high variance of reflectance values recorded in consecutive images meant that the thresholding of every image required an individual approach to obtain correct results. This, along with some degree of uncertainty regarding the identification of less dense accumulations, made the method unsuitable for automatic data processing (Kahru *et al.* 2007).

While only large concentrations may be identified visually, all floating algal colonies contain pigment chlorophyll which exhibits a peak in reflectance in the visible red channel (near 650 nm) and significantly lower reflectance in the near-infrared channels (around 750 nm). One of the oldest methods of finding pigment chlorophyll by exploiting this difference in reflectance is computing the Normalized Differential Vegetation Index (NDVI). Although the index was developed for the purpose of detecting vegetation over land (where it tends to form a similar peak in reflectance near 750 nm), over the years several researchers from around the world applied NDVI to manual detection of algal blooms with varying degrees of success (Kahru *et al.* 1993; Kutser 2004; Oyama *et al.* 2014), however the index has generally been found to be too sensitive to interference from aerosols and sun glint to produce a consistent time series (Hu *et al.* 2010). Thus, the results of quantitative NDVI-based microalgae detection always needed to be manually verified and corrected. Later research focused on techniques which took advantage of increased spectral resolution offered by sensors such as Moderate Resolution Imaging Spectroradiometer (MODIS), Medium Resolution Imaging Spectroradiometer (MERIS) and Sea-Viewing Wide Field-of-View Sensor (SeaWiFS). These sensors delivered substantially more spectral bands which in turn enabled instant verification of classification results, eg. by comparison to composite true colour images (Hu *et al.* 2010). Over the years they have been used to develop several methods of algae detection, including the maximum chlorophyll index, which relates the water-leaving reflectance at 709 nm to the value extrapolated from bands 681 nm and 753 nm (Gower *et al.* 2005), the floating algae index, which applies the same principle to the 859 nm, 645 nm and short-wave infrared bands (Hu 2009), and the cyanobacteria index, which detects cyanobacteria-specific reflectance ratios in the visible spectrum (Wynne *et al.* 2008).

The application of these methods to operational algal bloom detection and monitoring over the Baltic Sea is not straightforward, however. The main issue here is related to data availability. The Baltic is often clouded, which sometimes makes it problematic to find appropriate images for analysis. Out of the available satellite sensors, only AVHRR (installed on seven satellites: NOAA-15, 16, 17, 18 and NOAA-19 as well as MetOp-A and B) guarantees the delivery of several images of the Baltic during the daily hours. As far as the more advanced sensors are concerned, MODIS (limited to two satellites: Aqua and Terra) delivers on average a single image per day and Landsat satellites visit the region approximately once a week (Kahru, Elmgren 2014), while MERIS and SeaWiFS have been phased out entirely. Moreover, although dense clouds may be easily removed from a partially-clouded image, the remaining atmospheric artefacts such as water vapour significantly influence the recorded reflectance. For instance, the values of computed NDVI could be lower by as much as 0.1 for uncorrected data (Tanre *et al.* 1992), which could mean the difference between classifying a land-based pixel as vegetation or bare soil (Sobrino, Raissouni 2000). The various methods of identifying and removal of such artefacts are referred to as atmospheric correction, and involve extensive use of external reference data sources, such as sun photometers (Vermote *et al.* 1995; Fedosejevs *et al.* 2000), operational atmospheric radiance models (Trishchenko *et al.* 2002) and weather simulation models (Vermote *et al.* 2002). Thus far operational atmospheric correction methods which use data provided by the sensor itself have only been presented for the MODIS sensor, which offers high short-wave infrared resolution (Wang, Shi 2007; Okin, Gu 2015; Roy *et al.* 2014). This being said, the process of removing atmospheric artefacts from an image is a complex one, and even the availability of reliable reference data does not guarantee successful correction of the image. On the contrary, low signal-to-noise ratio of the input data or imprecise calibration of the correction algorithms may only result in introducing additional errors. (Kahru, Elmgren 2014) report that atmospheric correction of AVHRR data over the Baltic Sea often results in physically impossible negative values of water-leaving radiance, despite of the quality of used calibration coefficients. On the other hand, (Reinart, Kutser 2006) established

that standard algorithms for atmospheric correction, which employ the near-infrared and short-wave infrared bands of the MODIS sensor, often fail over the Baltic Sea, causing many pixels to be incorrectly flagged as erroneous. This is a particular problem during the microalgae blooming season, when high chlorophyll values generated by dense microalgae accumulations are removed from the image by the correction algorithms (Reinart, Kutser 2006).

Another problem with detecting microalgae is caused by the different spectral characteristics of deep and shallow waters. In particular, shallow coastal waters most often contain a high number of suspended organic matter. Because of this, they exhibit substantially higher spectral reflectance characteristics in comparison to clear open waters. In consequence, turbid and open waters must be processed differently even at the stage of atmospheric correction (Hu *et al.* 2000) and algorithms for detecting microalgae (which bloom primarily in open waters) most often mask out known turbid water regions (Kahru, Elmgren 2014).

It also should be noted that establishing the density of algal concentration is virtually impossible using remote sensing because microalgae can regulate their buoyancy and often create dense accumulations just below the opaque surface layer. Determining the actual amount of algae in such conditions is very difficult even when using a research vessel (because vessels disturb the natural distribution of phytoplankton). Thus, while remote sensing allows for mapping the location and extent of algal bloom, it should not be used to quantify its density (Metsamaa *et al.* 2006).

Aside from the issues with data availability and quality, it must also be noted that chlorophyll-a, although widely used as a marker of algal presence, is also found in other types of phytoplankton. Because of this, some researchers prefer to measure the amount of pigment phycocyanin (PC) which is characteristic for cyanobacteria (Ruiz-Verdu *et al.* 2008). Although satellite-based detection of PC requires analysis of spectral channels which are not provided by the AVHRR sensor, in-situ measurements of PC fluorescence can be applied to verification of algal blooms obtained from AVHRR satellite images. This is because cyanobacteria are characterized by much stronger backscattering in the 650 nm spectrum in comparison to other species of phytoplankton (Metsamaa *et al.* 2006; Ruiz-Verdu *et al.* 2008; Kahru, Elmgren 2014). Thus, the peak in reflectance near 650 nm may be detected via remote sensing even if the amount of cyanobacteria in biomass is as low as 15% (Metsamaa *et al.* 2006). Even if regular phytoplankton would form a swath dense enough to exhibit a similarly strong peak of reflectance, such a dense swath could only form during the blooming season of June-August. However, during the blooming season, cyanobacteria constitute between 72 and 94 percent of floating biomass in the Baltic Sea (Dekker *et al.* 1992). Thus analysis of strong peak reflectance in the upper visible spectrum accompanied with low infra-red reflectance, although theoretically typical for chlorophyll-a in general, is a widely accepted method of detecting harmful microalgae over both turbid (Randolph *et al.* 2008) and open waters (Reinart, Kutser 2006; Kahru, Elmgren 2014).

As far as operational monitoring of algal blooms in the Baltic Sea is concerned, there are several ongoing initiatives. The Baltic Algae Watch System (BAWS) is a web service maintained by the Swedish Meteorological and Hydrological Institute (SMHI) (SMHI BAWS 2016). The institute performs classification of satellite images from the MODIS sensor using the method by (Kahru *et al.* 2007) to identify surface and subsurface algal blooms by analysis of the normalized water-leaving radiances (nLw) in the 551 nm and 670 nm bands (Hansson, Hakansson 2007). The classification results are verified and commented on by an expert prior to being published online in the form of static images. Although very informative, the service does not allow any interaction with the presented data, and the produced images have a relatively small resolution. In parallel, the institute performs regular cruise vessel expeditions to the Baltic Proper which measure and describe water qualities such as oxygenation and presence of algal blooms. While the SMHI cruises are organized every 2–3 weeks, the Finnish Environment Institute (SYKE) provides similar data on a daily basis through the Alg@line initiative. Alg@line operates by equipping regular Baltic ferry ships with dedicated flow-through sensors (referred to as "Ferryboxes") which measure water salinity and turbidity as well as chlorohyll, phycocyanin and CDOM fluorescence. Built-in GPS receivers enable Ferryboxes to record the precise time and location of taken measurements, which are then made available online via a simple web mapping service (SYKE Algal Situation service 2016). The data is also available directly via a Web Feature Service provided by the FerryScope project (FerryScope WFS data service 2016). Although the in-situ measurements provided by Alg@line have very good temporal resolution, their scope is limited to the ferry lines ship routes, which omit large portions of the Baltic Proper including the Gulf of Riga, the Gulf of Gdansk, and most of the Eastern Gotland Basin (Kaitala 2016).

In-situ measurements are also provided by the International Council for the Exploration of the Sea (ICES) HELCOM network of Baltic Sea monitoring stations. The stations provide measurements of characteristics such as temperature, salinity and concentration of chlorophyll-a in different points of the basin. The HELCOM web page currently lists 730

available data sources, however not all of them are active simultaneously, and the availability of in-situ measurements for a given area and time period is not guaranteed (HELCOM data portal 2016).

To sum up, operational detection of algal blooms in the Baltic Sea is an endeavour that is both expensive and prone to error. First of all, the presently available remote sensing detection methods operate on MODIS data which may only be obtained through a very expensive X-Band Earth Observation System, or from third-party online services (eg. NASA Ocean Color: http://oceancolor.gsfc.nasa.gov). Secondly, the available services rely on quantitative image classification methods, which are highly dependant on the quality of the sensor's atmospheric correction. Moreover, the visualization functionalities of the currently available online systems do not provide even such basic user interaction features like zooming and panning. Finally, the low temporal resolution of the MODIS sensor, coupled with the usual weather conditions in the Baltic region often lead to large portions of the sea being obscured in the recorded satellite images. At the same time, available in-situ measurements are too limited either in scope (Alg@ line) or in time (HELCOM) to provide daily reports on the algae situation in the entire Baltic Sea basin.

In this context, the current situation could be improved by a system capable of unsupervised algae bloom detection using data provided by a sensor with a better temporal resolution than the one offered by MODIS. Providing the users with online tools for advanced analysis of the produced data, such as an interactive map with capabilities for zooming and panning over areas of interest and changing the colour scheme could prove to be even more beneficial.

This article presents a novel, non-quantitative and cost-effective method of operational detection of algal blooms in the Baltic Sea via a dedicated Geographic Information System for analysis of AVHRR data.

MATERIAL AND METHODS

The study area presented in this work encompasses the Baltic Sea from the Eastern half of the Arkona Basin in the West to the Southern part of the Gotland Basin in the North (Fig. 1).

The presented work uses satellite images recorded by the AVHRR sensor, which provides a spatial resolution of about 1.1 km and a spectral range which covers five channels. AVHRR observes the following parts of the electromagnetic spectrum (USGS AVHRR 2008):

- Band 1: 0.58–0.68 μm
- Band 2: 0.725–1.10 μm
- Band 3: 3.55–3.93 μm

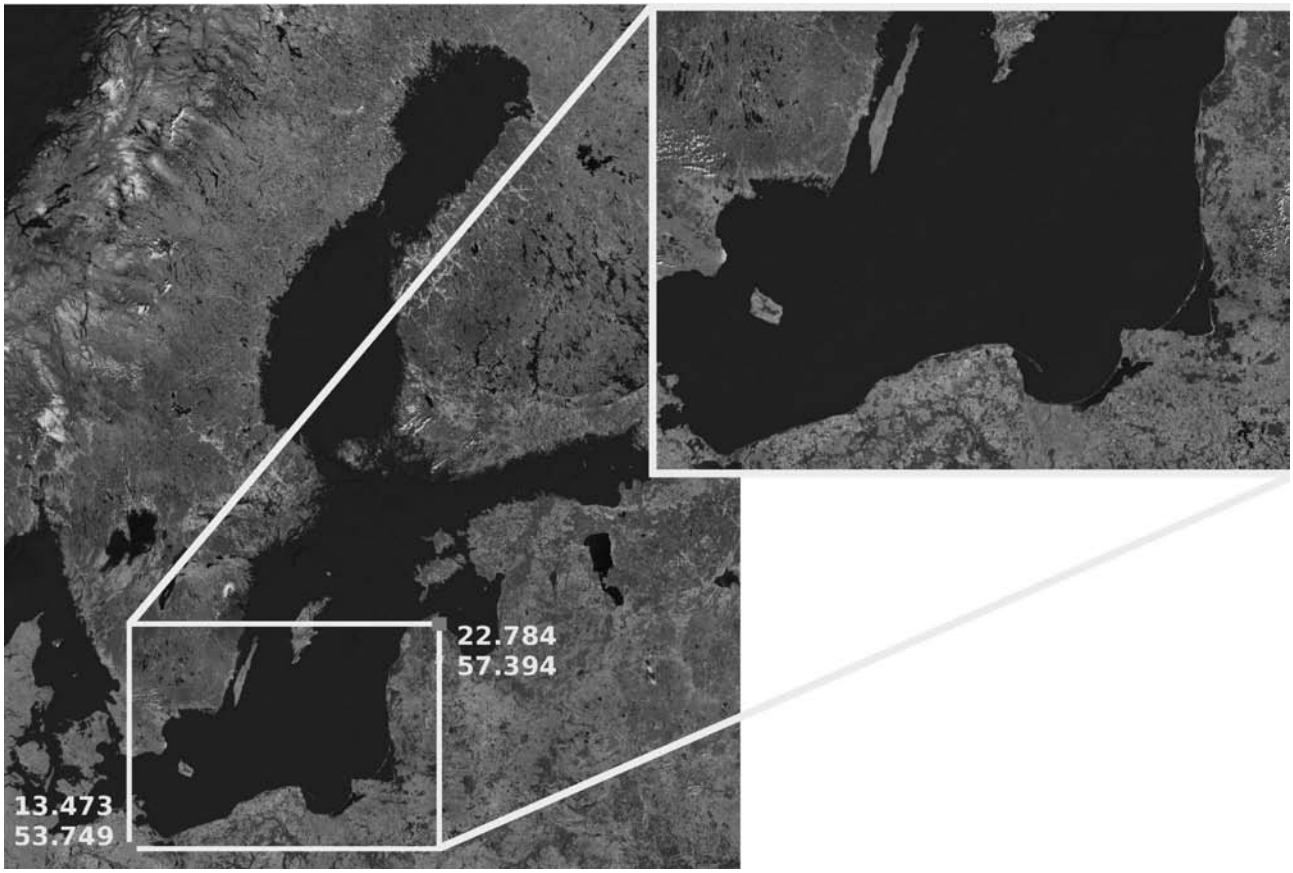

Fig. 1 The area of research encompasses the Southern Baltic Proper from the Eastern half of the Arkona Basin in the West to the Southern part of the Gotland Basin in the North

- Band 4: 10.50–11.50 μm
- Band 5: 11.5–12.5 μm

In the analysed region, the AVHRR sensor provides an average of seven images every 24 hours. After being cut down to the desired area, the images have a resolution of 1200 x 800 pixels.

As far as microalgae monitoring is concerned, the two first bands are most significant, as they represent the "Red" (visible) and "Near Infrared" (NIR) fragments of the spectrum. In particular, open water bodies generally exhibit high absorption in both the Red and NIR spectra, while according to Ahn *et al.* (1982), microalgae may be distinguished by high reflectance in the upper part of the visible (650–670 nm) spectrum, and low reflectance in the infrared (750 nm) spectrum. In particular, toxic microalgae such as cyanobacteria exhibit a higher peak reflectance at 650 nm in comparison to other types of floating phytoplankton (Kutser 2009).

While both past as well as currently employed methods of satellite-based microalgae bloom detection exploited the high reflectance in the visible (650 nm) band, automatic identification of algae colonies using AVHRR has been unsuccessful due to the variability in recorded spectral reflectance between consecutive images (Hu *et al.* 2010; Kahru, Elmgren 2014). In fact, universal threshold values identifying microalgae has been shown to be very problematic even for atmospherically corrected MODIS data (Kahru, Elmgren 2014).

Instead of looking for universal values of reflectance which would identify microalgae in every satellite image, the presented work concentrates on identifying high reflectance values in the 650 nm band by their comparison to the corresponding reflectance in the 750 nm band, individually for every satellite image. Because every satellite image is produced under different weather conditions, the difference in recorded spectral reflectance is best analysed after normalization. A well-known method of normalization the difference in spectral reflectance in the Red and NIR channels has been defined by Rouse *et al.* (1974):

$$\mathrm{NDVI} = (\mathrm{NIR} - \mathrm{RED})/(\mathrm{NIR} + \mathrm{RED}) \quad (1),$$

The possible values of NDVI fall in the range of (–1; 1). The index is particularly useful for identification of various features in satellite images. NDVI values in the range (–0.1; 1) typically describe various land surfaces (Justice *et al.* 1985; Roderick *et al.* 1996; Sobrino, Raissouni 2000). Moreover, NDVI values in the range (–0.1; 0.1) have also been shown to contain clouds (Simpson, Stitt 1998). Water surface is represented with near-zero values (–0.1; 0), while microalgae are characterized by NDVI values of –0.2 and lower (Ahn *et al.* 1982; Hu, He 2008). This remains true for both coastal and open waters, with the significant difference being the values of reflectance in both water types (Kutser 2009).

Theoretically, the analysis of NDVI histograms for satellite images captured outside of the algae blooming period should reveal a strong concentration of near-zero values representing clear water. Similarly, analysis of NDVI frequency distribution for images containing strong algae blooms should reveal a multi-modal (in the case of weak blooms, the near-zero mode would represent clear water) or unimodal (for strong blooms) histogram in the negative NDVI range. In both cases the mode representing microalgae would be located at the negative end of the NDVI distribution. Because NDVI values in the range (–0.1; 0) are known to contain water (Ahn *et al.* 1982) as well as clouds (Simpson, Stitt 1998), and the margin of error for NDVI values obtained from AVHRR (due to atmospheric interference) is known to be up to 0.1 (Tanre *et al.* 1992), the final NDVI interval in which microalgae might be identified without risking false positives would fall in the range of (–1; –0.2).

Mathematically, the proposed approach could be described as follows.

A pixel represents microalgae if its NDVI value (c_{NDVI}) falls in the range:

$c_{NDVI} \in (-1, ..., x_{\mathrm{mode}})$,

where the modal value x_{mode} is given by:

$$X_{\mathrm{mode}} = r_k + \left(\frac{f_n(k+1, X)}{f_n(k-1, X) + f_n(k+1, X)} \right) (r_{k+1} - r_k) . \quad (2)$$

In the above equation:

$f_n(j, X) = \frac{1}{|X|} \sum_{x_j \in X} 1\{x_i \in (r_j, r_{j+1})\}$ represents all NDVI values within the range (r_j, r_{j+1}),

$f_n(k, X) = max\, f_n(j, X), j = 1, ..., K$ is the modal interval of the NDVI frequency analysis,

X represents the set of samples $(x_1, ... x_n)$,

K denotes the number of analysed intervals, and

r_k is the lower boundary of the k interval.

The presented algorithm has been implemented as part of an operational system for microalgae bloom detection in the Baltic Sea (Fig. 2). The main source of data for the presented system is a 1.5m-wide HRPT/MetOp-A/B local satellite ground station operated by the Gdansk University of Technology Faculty of Electronics, Telecommunications and Informatics in Gdansk, Poland. The station downloads data in real-time from overpassing AVHRR satellites via the High Rate Picture Transmission (HRPT) stream (Moszynski *et al.* 2015).

The images captured by the satellite ground station are automatically processed by the Dartcom iDAP module, which puts together lines of the HRPT stream

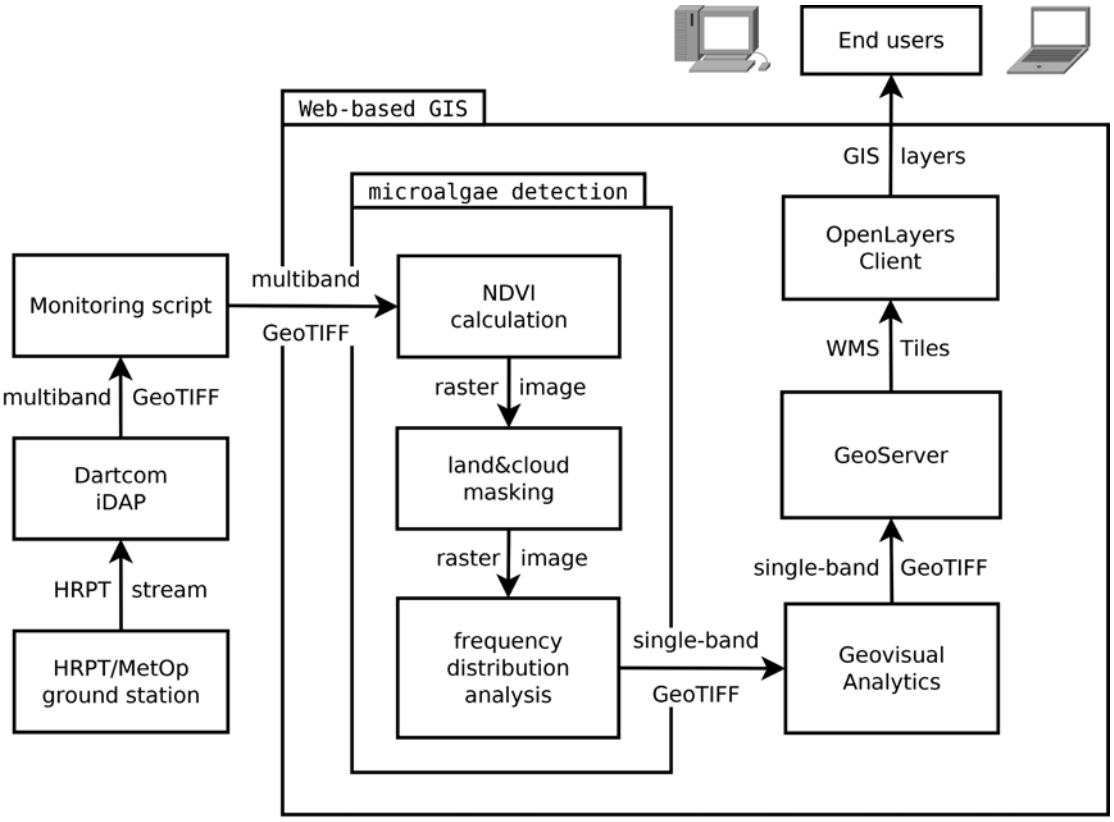

Fig. 2 Architecture of the Web-GIS for operational microalgae detection

to form images. The software is configured to convert the obtained images into multiband GeoTIFF files after basic processing involving masking out missing lines of data. Every time a new GeoTIFF file arrives, it is automatically detected by a monitoring script which passes it to the microalgae detection module. The microalgae detection module consists of several sub-modules built with the Open Source GeoTools library. The GeoTIFF is first processed by the NDVI calculation sub-module, which extracts raw AVHRR bands 1 (0.58–0.68 μm) and 2 (0.725–1.0 μm) from the file and uses them to compute NDVI for the entire image. The resulting single-band raster is passed on to the land&cloud masking sub-module, which removes all pixels with NDVI values larger than –0.2. The resulting raster is passed on to the frequency distribution sub-module, which finds the maximum and minimum NDVI values in the image and computes a 256-bin histogram. The module then finds the mode of negative NDVI distribution. In order to avoid possible errors caused by local variations in recorded spectral reflectance, the histogram mode is only accepted if it contains at least 0.5% of all pixels in the analysed image (for the images used in this study, this corresponds to a value of 5000 pixels). The microalgae detection module produces single band GeoTIFF images which contain the detected microalgae accumulations represented by values of negative NDVI found between the histogram mode and the smallest detected value of NDVI. Images in this form are then processed by the Geovisual Analytics module, which performs their adaptive palette matching for the purpose of pixel value normalization. The name of the module refers to the field of science which deals with solving geographic problems requiring analytical reasoning and dissemination of information to a variety of audiences (Andrienko *et al.* 2007; Kulawiak, Lubniewski 2013). For every image, the Geovisual Analytics module produces two distinct colour palettes in the form of Open Geospatial Consortium (OGC) Styled Layer Descriptor (SLD) files. The default palette is meant to present the general shape of the algae colony, while the alternate one is dedicated to providing a better contrast between individual NDVI values in the bloom area. This allows for individual analysis of every image via dynamic palette swapping at the visualization stage through the client module of the system. The SLD and GeoTIFF images are then registered in the GeoServer module, which is an Open Source Web Map server with excellent support for open standards of data exchange and dissemination. It supports a variety of raster and vector data formats, such as Shapefile, SVG, KML, GML, GeoTIFF, JPG, PNG or PostGIS, allows for their individual styling using SLD files, and enables their Web-based presentation through open protocols such as OGC Web Map Service (WMS), Web Feature Service (WFS) or Web Coverage Service (WCS). Once the GeoTIFF images

have been registered in the GeoServer database, they are remotely accessible to clients through the WMS protocol. The presented system provides users with a Web client built in DHTML using the Open Source OpenLayers library. OpenLayers allows for the construction of interactive GIS applications for display and manipulation of vector and raster geospatial data, which can be obtained from external sources through standard protocols such as WMS and WFS. Because OpenLayers is written in pure Javascript, it is easily integrated with Javascript frameworks such as Ext. js, allowing for building advanced GIS functionalities with rich Graphical User Interface (GUI), which run in any standard-compliant Web browser without the need to install plug-ins. The OpenLayers client allows end users to browse the detected microalgae accumulations in the form of thematic layers overlaid on satellite images of the Baltic Sea basin. Aside from standard operations like zooming, panning and changing the visibility of individual layers, the OpenLayers client also enables the user to apply alternative colouring palettes (via the 'styles' part of the WMS GetMap request) to every microalgae layer in real-time.

The presented system has been applied to detection of microalgae in the Baltic Sea during the blooming periods of 2013 and 2014. According to the reports from SMHI vessel cruises, the 2013 microalgae blooms started in late June and lasted through July (Thell 2013b; Thell 2013c). This is confirmed by ship transects from Alg@line vessels, which show a rapid drop in phycocyanin (PC) reflectance recorded in the Baltic Proper between 27.07.2013 and 04.08.2013 (FerryScope WFS data service 2016). In 2014, the SMHI cruise vessels reported sightings of algae colonies in the second half of June as well as July and August (Thell 2014; Andersson 2014). The Alg@ line measurements also show heightened PC reflectance during this time period, however unlike in the previous year, the PC values show greater variability which indicates more dynamic changes on the surface of the bloom.

Basing on those reports, the periods of 15.06.2013–31.08.2013 and 15.06.2014–31.08.2014 (a total of 156 days) were selected for investigation. During this time, the AVHRR station received and stored 1018 images. 363 out of which were captured in the time span between 10:00 UTC and 15:00 UTC (which provides best solar irradiance of the Baltic). Due to bad weather conditions, 140 of those images were completely clouded in the analysed area, while 113 exhibit cloud cover in the range 60%–80%. In the end, out of 110 images captured on 44 days of good weather, one best image for each day was used in the presented work.

For the purpose of verification, the results obtained via the presented methodology have been compared in-situ measurements of phycocyanin reflectance along the Travemuende-Helsinki and Travemuende-Kemi ferry routes performed by SYKE Ferrybox vessels in the scope of the FerryScope project (FerryScope WFS data service 2016). In the selected time period, the FerryScope data service provides measurements on 49 days, which can be matched to 13 satellite images captured on days with good weather conditions. In order to provide reference data for other satellite images, in-situ chlorophyll-a measurements obtained from the HELCOM data portal (HELCOM data portal 2016) have also been used. In the selected time period there are only 18 days during which the HELCOM stations provide measurements form more than one station. After aggregation, these measurements may be used as reference data for five satellite images captured in good weather conditions.

For additional optical verification, the study uses algae concentration assessments produced by SMHI through classification of MODIS data using the method by (Kahru *et al.* 2007), as well as true-colour MODIS Aqua images supplied by NASA through the agency's Ocean Color website (http://oceancolor.gsfc.nasa.gov). The results of these comparisons are presented in the following section.

RESULTS

This section presents the microalgae colonies detected by the presented system. The algae concentrations are presented in the form of WMS layers overlaid on background satellite images of the Baltic (Fig. 3; Fig. 4). Every figure also contains an additional layer which represents reference in-situ measurements of phycocyanin fluorescence or chlorophyll-a values for the time period matching the day the satellite image was recorded. The mean value of chlorophyll-a concentration in the analysed area in the period of 01.01.2013–31.12.2014 is 2.46 µg/L, while the median value is 1.69 µg/L. The mean value of recorded PC fluorescence for the period of 20.03.2014–27.08.2014 is 0.08, and the first non-zero values in that period have been recorded on 05.06.2014. Scatterplots of PC fluorescence against AVHRR NDVI are also present for dates on which more than 20 PC measurements could be matched to corresponding NDVI values.

The detected algae concentrations are presented according to the two colour schemes provided by the client module of the Web GIS. In the default mode, the extent of microalgae is depicted by colour, while the variance in detected surface accumulation is represented by intensity. The alternate display mode employs a false-colour representation in which the detected variance in microalgae accumulation is depicted using a dedicated colour gradient. In this mode red colour represents the highest detected negative

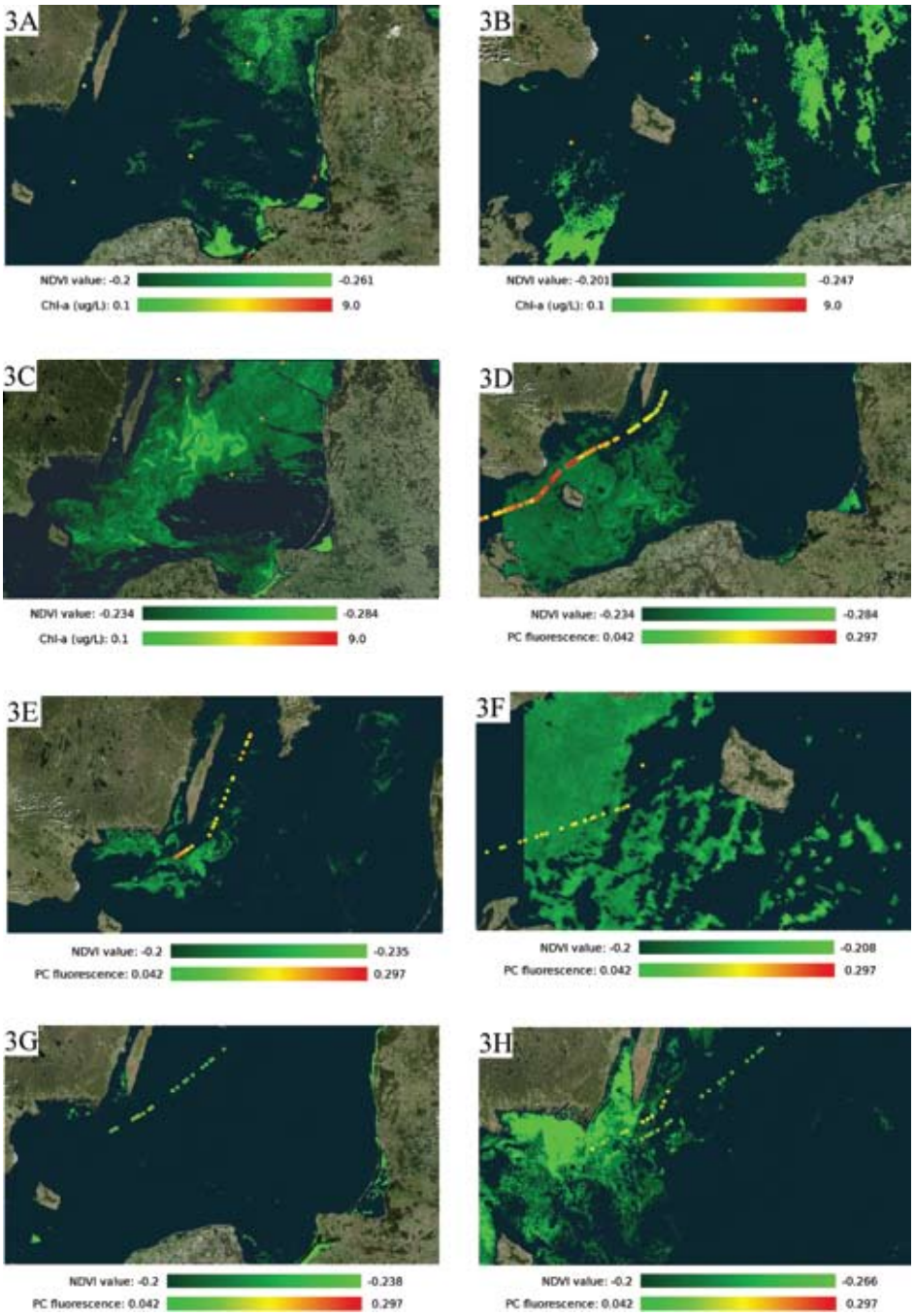

Fig. 3A-3C. In-situ measurements from HELCOM stations: A. Recorded in the period between 2013.06.17 and 2013.06.18 overlaid on a microalgae colony detected in the AVHRR image captured on 2013.06.18. The chlorophyll-a values range from 1.3 µg/L West of Oland to 5.16 µg/L in the Bay of Gdansk. The applied colour scale does not include the value of 47.5 µg/L, which was recorded in the Vistula Lagoon (bottom of map). **B.** Recorded in the period between 2013.06.24 and 2013.06.27 overlaid on a microalgae colony detected in the AVHRR image captured on 2013.06.24. The chlorophyll-a values range from 3.3 µg/L to 3.9 µg/L. **C.** Recorded in the period between 2013.07.15 and 2013.07.17 overlaid on a microalgae colony detected in the AVHRR image captured on 2013.07.17. The chlorophyll-a values range from 2.3 µg/L to 4.1 µg/L. **Fig. 3D-3H. In-situ measurements from Ferrybox vessels: D.** Recorded in the period between 2013.07.20 and 2013.07.21 overlaid on a microalgae colony detected in the AVHRR image captured on 2013.07.21. The PC fluorescence values range from 0.098 to 0.246. **E.** Recorded in the period between 2013.07.24 and 2013.07.25 overlaid on a microalgae colony detected in the AVHRR image captured on 2013.07.24. The PC fluorescence values range from 0.116 to 0.152. **F.** Recorded in the period between 2013.07.27 and 2013.07.31 overlaid on a microalgae colony detected in the AVHRR image captured on 2013.07.31. The PC fluorescence values range from 0.09 in the Arkona Basin to 0.297 in the Baltic Proper. **G.** Recorded on the period between 2013.08.01 and 2013.08.02 overlaid on a microalgae colony detected in the AVHRR image captured on 2013.08.01. The PC fluorescence values range from 0.052 to 0.088. **H.** Recorded in the period between 2013.08.01 and 2013.08.03 overlaid on a microalgae colony detected in the AVHRR image captured on 2013.08.03. The PC fluorescence values range from 0.052 to 0.155

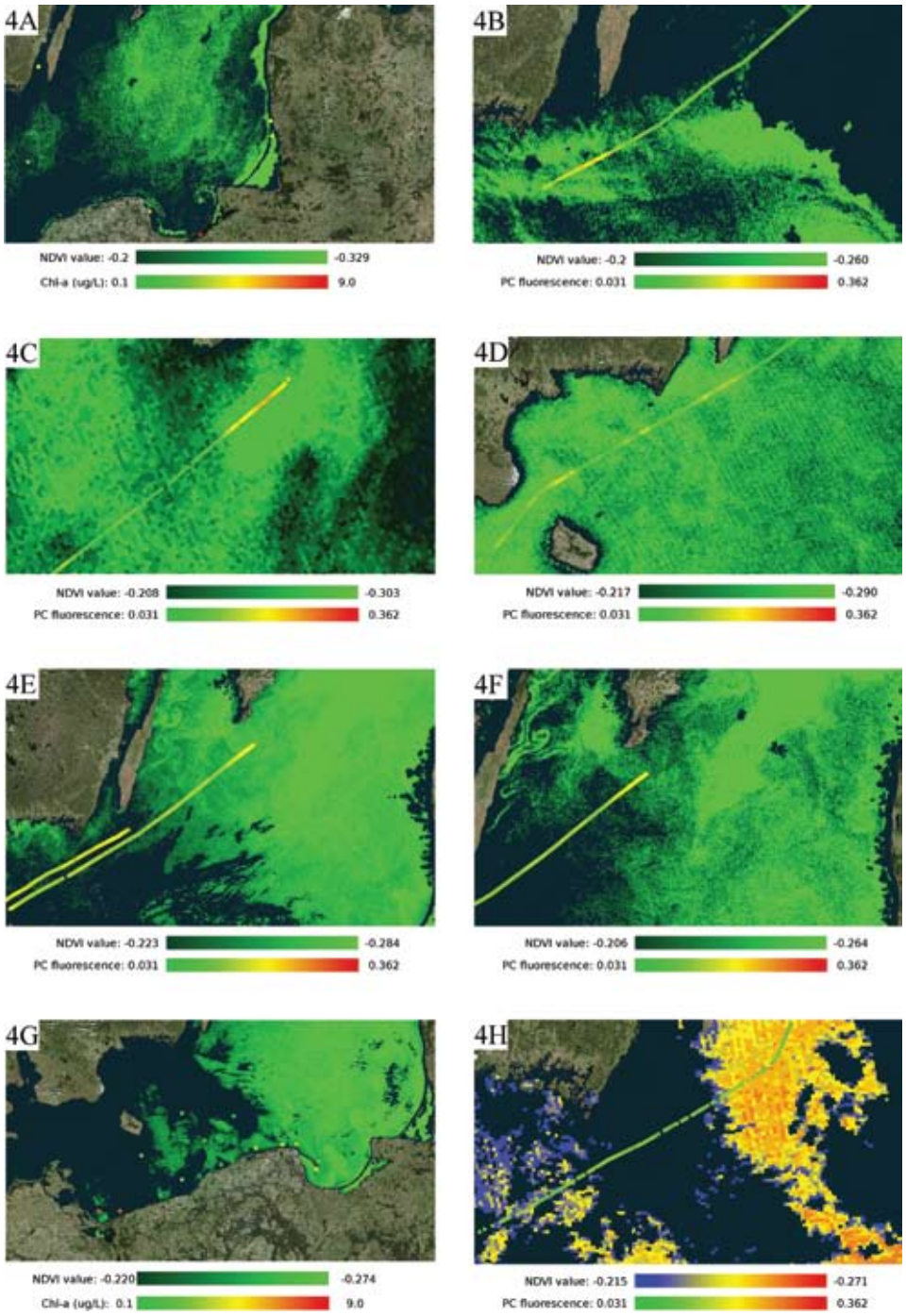

Fig. 4A, 4G. In-situ measurements from HELCOM stations: A. Recorded in the period between 2014.06.11 and 2014.06.19 overlaid on a microalgae colony detected in the AVHRR image captured on 2014.06.15. The chlorophyll-a values range from 0.1 µg/L East of Oland to 3.28 µg/L in the Bay of Gdansk. The applied colour scale does not include the value of 38.6 µg/L, which was recorded in the Vistula Lagoon (bottom of map). **G.** Recorded in the period between 2014.08.06 and 2014.08.08 overlaid on a microalgae colony detected in the AVHRR image captured on 2014.08.07. The chlorophyll-a values range from 1.13 µg/L to 5.75 µg/L. **Fig. 4B-4F, 4H. In-situ measurements from Ferrybox vessels: B.** Recorded on 2014.07.04 overlaid on a microalgae colony detected in the AVHRR image captured on 2014.07.04. The PC fluorescence values range from 0.10 to 0.197. **C.** Recorded South of Gotland on 2014.07.07 overlaid on a microalgae colony detected in the AVHRR image captured on 2014.07.07. The PC fluorescence values range from 0.078 to 0.286. **D.** Recorded in the period between 2014.07.08 and 2014.07.09 overlaid on a microalgae colony detected in the AVHRR image captured on 2014.07.09. The PC fluorescence values range from 0.09 to 0.161. **E.** Recorded in the period between 2014.07.21 and 2014.07.22 overlaid on a microalgae colony detected in the AVHRR image captured on 2014.07.21. The PC fluorescence values range from 0.12 to 0.194. **F.** Recorded on 2014.07.22 overlaid on a microalgae colony detected in the AVHRR image captured on 2014.07.22. The PC fluorescence values range from 0.12 to 0.194. **H.** Recorded in the period between 2014.08.15 and 2014.08.16 overlaid on a microalgae colony detected in the AVHRR image captured on 2014.08.15. The PC fluorescence values range from 0.11 to 0.135

NDVI values, while lower negative NDVI values are represented by hues of orange, yellow and blue respectively. This functionality is particularly useful when detailed analysis of particular algae colonies is required, for example when investigating whether the outline of a detected colony is a product of cloud masking. As it can be seen (Fig. 4H), the application of this colour scheme to the colony detected on 15.08.2014 not only allows for better contrast against the reference Alg@line data, but also reveals a sharp rise of NDVI values on the borders of the microalgae colony. The sharp change in NDVI values is an artefact caused by thin cirrus clouds which were not completely removed on the land&cloud masking stage.

During the presented research it was discovered that although the values of negative NDVI for images captured in similar time periods and environmental conditions (sunny days with clear skies) can vary by more than 18%, which may be observed eg. on images captured on 21.07.2014 and 22.07.2014 (Fig. 4E and 4F), the frequency distribution of NDVI remains largely similar. This may be analysed by examining eg. the negative NDVI histograms for satellite images captured on 07.07.2014 and 09.07.2014 (Fig. 5).

The histograms on both images share a similar shape, however the histogram mode on the left image is –0.208 and the smallest NDVI value is –0.303. In the second image, taken only two days later, the histogram mode is the value of –0.217 and the smallest recorded value is –0.290. The situation has been found to be similar for the entire time series of analysed images. The comparison of NDVI frequency distribution for water surface always reveals a unimodal histogram, however the characteristics of these distributions (such as frequency, mean, median and mode) tend to differ to varying degrees. This may be further analysed on scatterplots of NDVI values against their matching PC fluorescence measurements (Fig. 6).

A comparison of microalgae bloom detection results produced by the presented method with true colour images from the MODIS sensor and the results of their classification performed by SMHI on six sample days with best weather conditions, chosen from the analysed blooming periods (Fig. 7). The first column of the figure contains atmospherically corrected true colour satellite images captured by the MODIS sensor for the given date, the third column contains the results of their classification using the method by (Kahru *et al.* 2007) (orange colour represents microalgae, yellow represents subsurface blooms and grey marks the cloud mask) while the second column contains results produced by the presented system on an AVHRR image that was closest in time to the MODIS captures.

While scenes recorded in good weather conditions are analysed properly by both methods, during the presented research it has been found that on cloudy days the theoretically superior temporal resolution of AVHRR occasionally produces practical advantages over MODIS. In particular, exploration of NASA MODIS online archives for the analysed periods revealed many situations in which the Baltic Proper is 85–95% clouded in the MODIS images. At the same time, images which were recorded by AVHRR sensors an hour earlier (rarely an hour-two later) may produce significantly improved visibility of the same area. Such situations may be observed eg. on 14.07.2013, 28.07.2013 and 03.07.2014.

It should be noted that past research occasionally employed comparisons to other types of reference data, such as MODIS Level 2 chlorophyll products. However, the analysis conducted for the purposes of this research revealed that the overly aggressive atmospheric correction applied by MODIS Level 2 processing algorithms often removes the highest chlorophyll accumulations, making the products

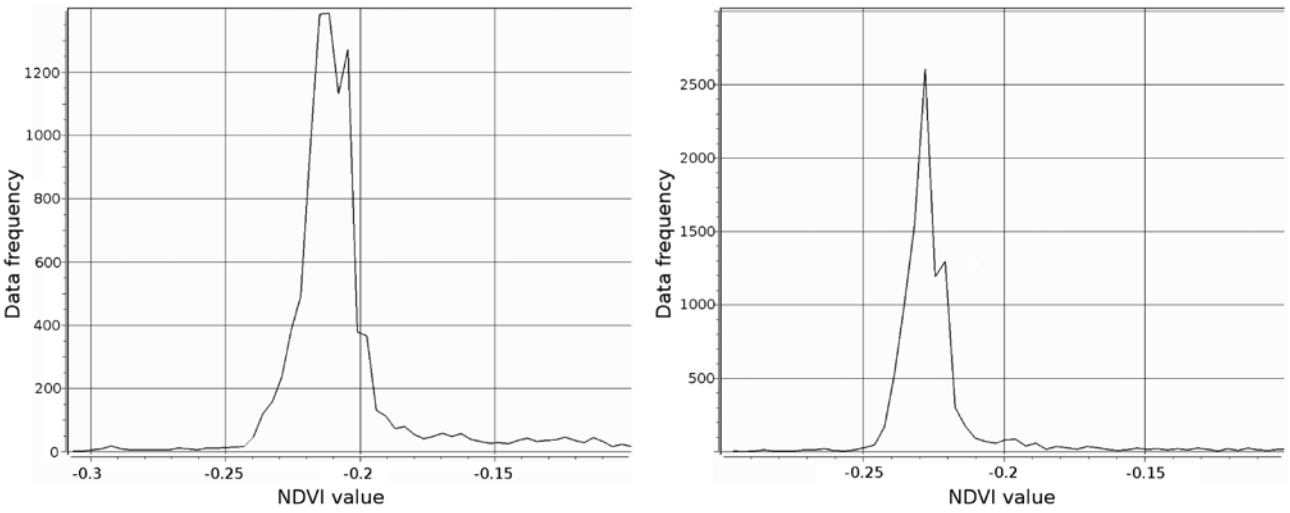

Fig. 5 Negative NDVI frequency distribution for AVHRR images captured on 07.07.2014 11:25 UTC (left) and 09.07.2014 11:03 UTC (right)

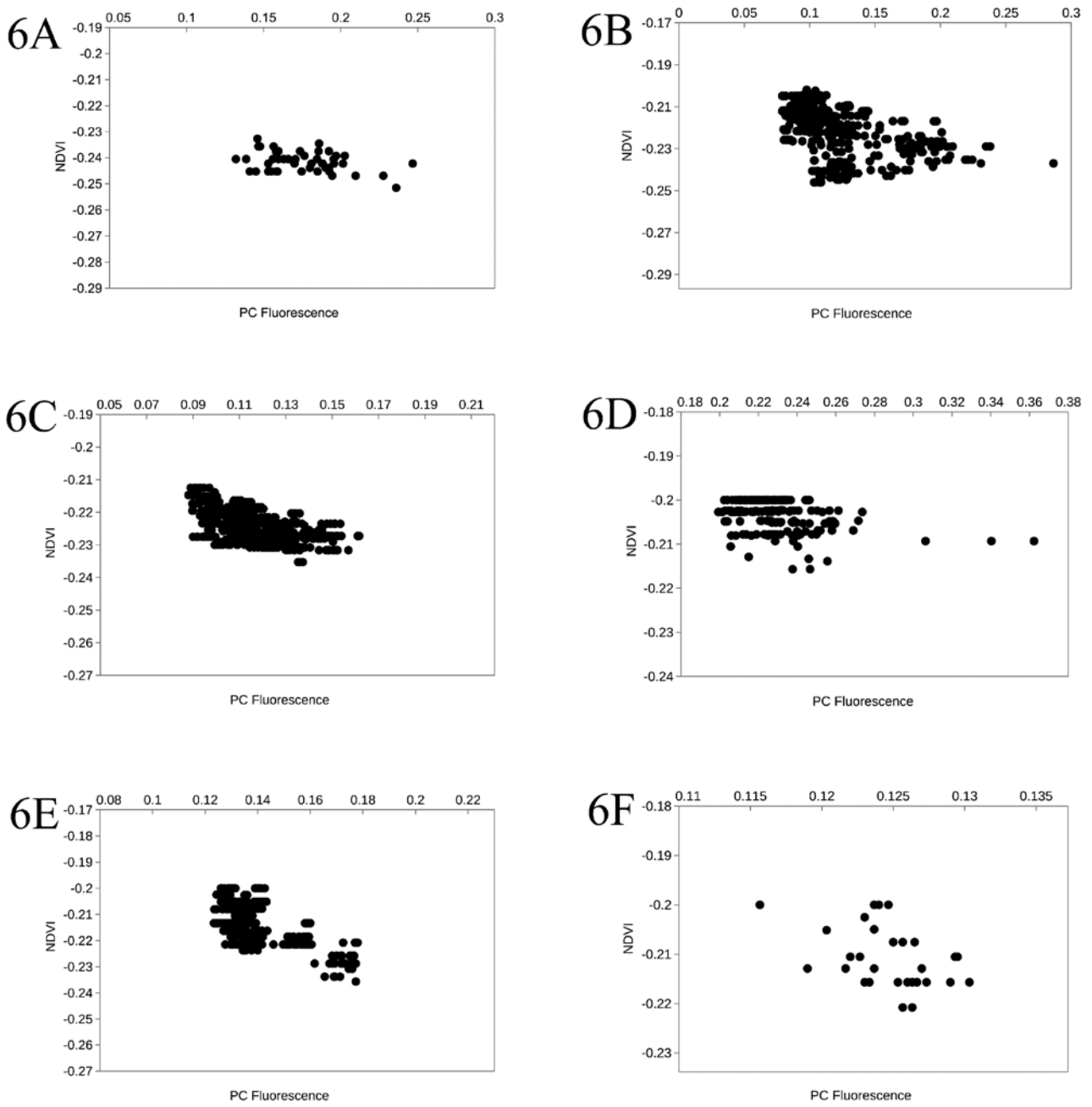

Fig. 6A-6F Scatterplot of NDVI values obtained from AVHRR image against corresponding in-situ PC fluorescence measurements. **A.** Recorded on 21.07.2013. **B.** Recorded on 07.07.2014. **C.** Recorded on 09.07.2014. **D.** Recorded on 16.07.2014. **E.** Recorded on 21.07.2014. **F.** Recorded on 15.08.2014

unsuitable for reference comparisons. This also means that the MODIS atmospheric correction algorithms have not been improved since (Reinart, Kutser 2006) documented this issue nearly a decade ago.

DISCUSSION

The proposed method has proven to properly detect surface colonies of harmful microalgae such as cyanobacteria. The presented results (see Fig. 3 and Fig. 4) indicate that the microalgae spatial concentrations detected using the proposed method in general correspond well to higher than average PC flouresсence levels, as recorded by the Ferrybox vessels. In most cases the appearance of dense clouds makes it impossible to observe the relationship of PC fluorescence levels to the NDVI values along the entire vessel transect, however the good weather conditions on 21.07.2013 (see Fig. 3D), 07.07.2014 (see Fig. 4C), 09.07.2014 (see Fig. 4D), 21.07.2014 (see Fig. 4E) and 15.08.2014 (see Fig. 4H) indicate a possible correlation between the value of negative NDVI and the density of detected microalgae colony. While the change in PC and NDVI values of those scenes

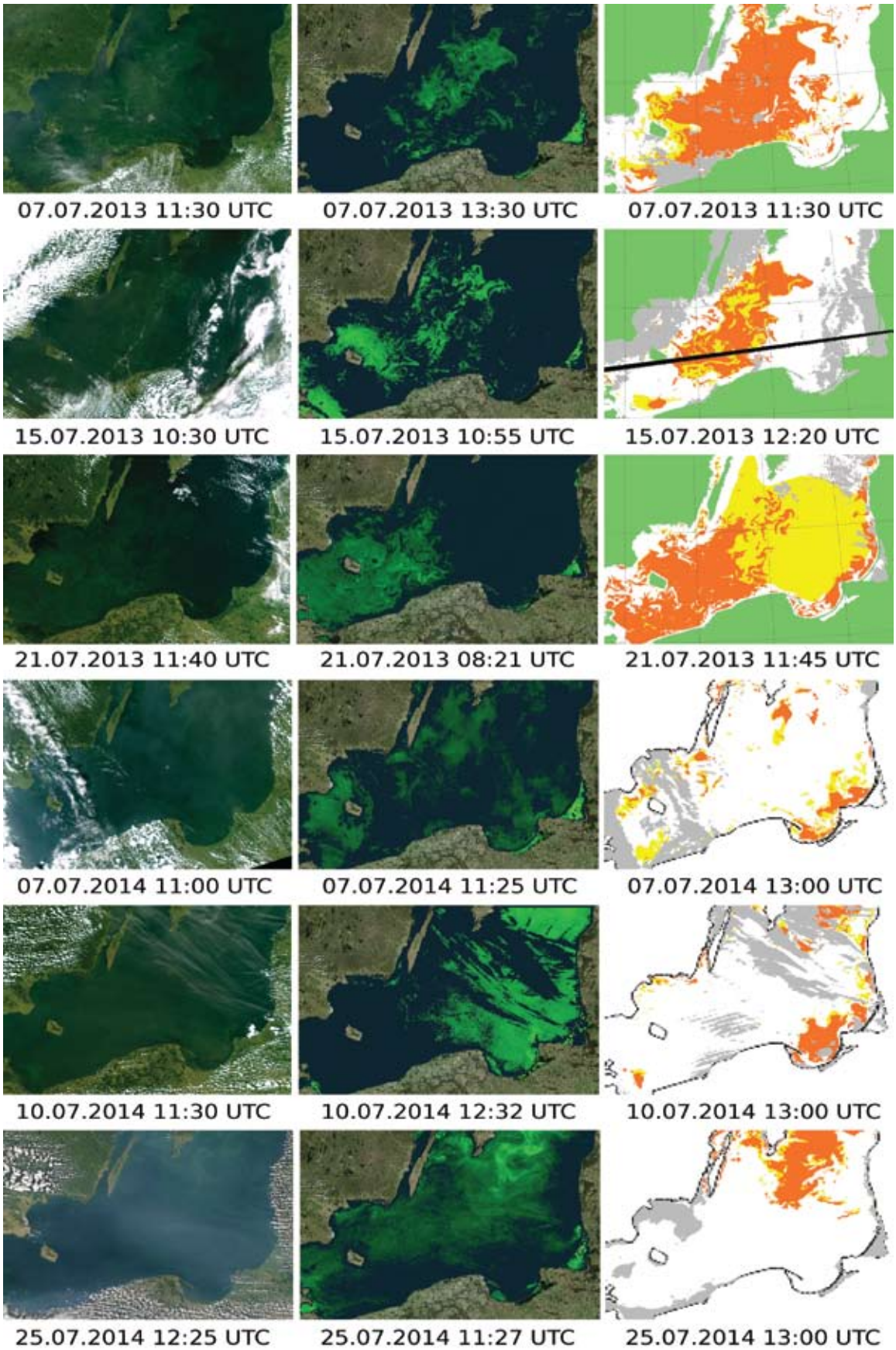

Fig. 7 Comparison of the obtained AVHRR-based microalgae detection results (centre) with algae situation analysis by SMHI performed on MODIS data (right) and a true-colour MODIS image (left). Variation in algae accumulation is depicted by colour intensity. In SMHI images microalgae are represented with orange colour, while yellow represents subsurface blooms

generally approaches a linear characteristic (see Fig. 5), unfortunately the high variance in NDVI values obtained from consecutive images does not allow to apply the presented method for estimation of quantitative values of microalgae colony density. It should be noted, however, that the comparison of obtained results with in-situ Alg@line measurements has not revealed any false positives. As it can be seen eg. on 01.08.2013 (see Fig. 3G), the lack of detected microalgae concentrations south of Oland correlates with very low recorded PC fluorescence (average value of 0.05).

As far as comparisons to other sources of reference data are concerned, it must be said that despite the large number of available stations, the number of actual in-situ measurements provided by the ICES HELCOM stations for the analysed area and time period was relatively small. Even including the measurements made in the same week only allowed to match a maximum of seven stations to any given image. This being said, although the station locations rarely directly overlap with detected microalgae colonies, they all show higher than average chlorophyll-a concentration in the area of the identified blooms.

The comparison of results produced by the proposed method with those obtained with the only alternative remote sensing method of Baltic Sea algae detection (see Fig. 7) reveals that the microalgae colonies identified by both methods are similar in shape and extent. Also, the extent of the algal bloom which may be discerned in the true-colour satellite images is similar or larger than the areas identified by either method. This is likely due to the aggressiveness of applied cloud screening algorithms, as close inspection suggests that the areas in question (eg. South-Western part of the satellite image from 07.07.2013 or the central area of the satellite image from 25.07.2014) may contain a thin semi-transparent cloud layer which could influence the accuracy of detecting underlying algal blooms. It should also be noted that because the time difference between images produced by MODIS and AVHRR varies between twenty five minutes and three hours, some of the differences observed between the images may also be caused by a variance in cloud cover.

The differences in results obtained by the presented system and the SMHI service may be caused by several factors. First of all, the higher spectral resolution of the MODIS sensor has enabled SMHI to identify subsurface blooms by analysing water column scattering in the 551 nm band. Thus the SMHI images differentiate detected microalgae into floating (represented by orange colour) and submerged (coloured in yellow). Other differences may be caused by a variance in sensitivity of both algorithms. For example, examination of reference true colour MODIS images (see Fig. 7) suggests that certain areas which were classified as "clean" by the SMHI method (eg. South of Gotland on 10.07.2014 or North of Bornholm on 25.07.2014) do contain some amounts of floating organisms as indicated by results obtained via the presented algorithm, while some other cases (South of Bornholm on 07.07.2014) show an opposite situation. However, these differences may also be caused by the lack of atmospheric correction in the AVHRR images, overly aggressive atmospheric correction parameters applied to the MODIS images, or simply a different arrangement of opaque clouds at the time of image capture.

Other differences in results obtained by the MODIS image classification employed by SMHI and the results produced by the presented algorithm include the treatment of shallow water areas such as the Vistula and Curonian Lagoons visible in the lower right part of the presented images. In particular, because shallow waters tend to produce higher spectral reflectance than open waters (which adversely affects the performance of a quantitative classification algorithm), SMHI chose to to remove those areas from their images prior to publishing. However, it is not unknown for harmful algae to flourish in shallow waters. For instance, cyanobacteria has been known to regularly bloom in the Curonian Lagoon (Alexandrov 2010; Paldaviciene *et al.* 2010) while *Microcystis aeruginosa* has also been found in water samples from the Vistula Lagoon (Mazur-Marzec *et al.* 2010). (Kutser *et al.* 2006) have shown that the general reflectance characteristics of harmful algae in visible and near-infrared spectra are similar in both turbid and open waters. Since the presented algorithm analyses the frequency distribution of spectral reflectance instead of its value, it should be more resistant to classification errors introduced by turbid waters. Because of this, coastal water areas are preserved in the final images, although the accuracy of results obtained by the presented method for turbid waters requires further research.

CONCLUSIONS

The comparison of results produced by the proposed Baltic Sea microalgae detection method to in-situ measurements obtained during the blooming seasons of 2013 and 2014 suggests that low negative values of normalized difference in reflectance between the visible and near-infrared spectral bands are correlated with elevated PC fluorescence levels. The results also indicate that the products of the proposed algorithm are comparable to those obtained from the MODIS sensor, which provides higher spectral and temporal resolution but lower availability. The conducted analysis was automated within a dedicated GIS

for operational Web-based analysis and visualization of processed satellite data in a geographical context. By operating on AVHRR data obtained directly from a satellite ground station, the presented solution provides an integrated and cost-effective means of continuous monitoring of the Baltic Sea, while ensuring the highest availability of remote sensing data as well as independence from third-party services. As a consequence, the integration of the algorithm for unsupervised data classification with operational software for data analysis and dissemination of results constitutes an automated tool for detection and monitoring of microalgae blooms in marine environments.

ACKNOWLEDGEMENTS

The author would like to thank the referees for their invaluable suggestions and recommendations. The presented reference algae detection results based on the MODIS sensor are reproduced with permission from the Swedish Meteorological and Hydrological Institute. The presented reference in-situ measurements were performed in the scope of the FerryScope project (ferryscope.org). The reference MODIS images have been obtained from the NASA OceanColor online repository (http://oceancolor.gsfc.nasa.gov).

REFERENCES

Ahn, Y.-H., Bricaud, A., Morel, A., 1992. Light backscattering efficiency and related properties of some phytoplankters. *Deep-Sea Research 39*, 1835–1855.

Aleksandrov, S. V., 2010. Biological production and eutrophication of Baltic Sea estuarine ecosystems: the Curonian and Vistula Lagoons. *Marine Pollution Bulletin 61 (4)*, 205–210.

Andersson, L., 2014. Cruise report from R/V Aranda week 32, 2014. Swedish Meteorological and Hydrological Institute. Source: http://www.smhi.se/en/publications/cruise-reports-from-the-marine-monitoring/cruise-report-from-r-v-aranda-week-32-2014-1.77360 [Accessed on 19.04.2016].

Andrienko, G., Andrienko, N., Jankowski, P., Keim, D., Kraak, M. J., MacEachren, A., Wrobel, S., 2007. Geovisual analytics for spatial decision support: Setting the research agenda. *International Journal of Geographical Information Science 21 (8)*, 839–857.

Dekker, A.G., Malthus, T.J., Goddijn, L.M., 1992, November. Monitoring cyanobacteria in eutrophic waters using airborne imaging spectroscopy and multispectral remote sensing systems. Proceedings of Sixth Australasian Remote Sensing Conference 1, 204–214

Dodds, W. K., Bouska, W.W., Eitzmann, J. L., Pilger, T. J., Pitts, K. L., Riley, A. J., Schloesser, J.T., Thornbrugh, D.J., 2009. Eutrophication of U.S. freshwaters: Analysis of potential economic damages. *Environmental Science & Technology 43 (1)*, 12–19.

Falconer, I.R., Beresford, A.M., Runnegar, M.T., 1983. Evidence of liver damage by toxin from a bloom of the blue-green alga, *Microcystis aeruginosa*. *The Medical Journal of Australia 1 (11)*, 511–514.

Fedosejevs, G., O'Neill, N. T., Royer, A., Teillet, P. M., Bokoye, A. I., McArthur, B., 2000. Aerosol optical depth for atmospheric correction of AVHRR composite data. *Canadian Journal of Remote Sensing 26 (4)*, 273–284.

FerryScope WFS data service, 2016. Finnish Environment Institute. Source: http://ferryscope.ymparisto.fi/Rflex/services/RflexWFS [Accessed on 19.04.2016].

Filella, I., Penuelas, J., 1994. The red edge position and shape as indicators of plant chlorophyll content, biomass and hydric status. *International Journal of Remote Sensing 15 (7)*, 1459–1470.

Glibert, P.M., Anderson, D.M., Gentien, P., Graneli, E., Sellner, K.G., 2005. The global, complex phenomena of harmful algal blooms. *Oceanography 18 (2)*, 136–147.

Gower, J., King, S., Borstad, G., Brown, G., 2005. Detection of intense plankton blooms using the 709 nm band of the MERIS imaging spectrometer. *International Journal of Remote Sensing 26 (9)*, 2005–2012.

Havens, K. E., 2007. Cyanobacteria blooms: Effects on aquatic ecosystems. In H. K. Hudnell (Ed.), Proceedings of the Interagency, International Symposium on Cyanobacterial Harmful Algal Blooms (ISOC-HAB): State Of The Science And Research Needs. Springer, New York, 733–747.

Hansson, M. Hakansson, B., 2007. The Baltic Algae Watch System-a remote sensing application for monitoring cyanobacterial blooms in the Baltic Sea. *Journal of Applied Remote Sensing 1 (1)*, 011507, http://doi.org/10.1117/1.2834769

HELCOM data portal. 2016. International Council for the Exploration of the Sea (ICES). Source: http://ocean.ices.dk/helcom/Helcom.aspx [Accessed on 22.04.2016]

Hu, C., Carder, K. L., Muller-Karger, F. E., 2000. Atmospheric correction of SeaWiFS imagery over turbid coastal waters: a practical method. *Remote sensing of Environment 74 (2)*, 195–206.

Hu, C., He, M. X., 2008. Origin and offshore extent of floating algae in Olympic sailing area. Eos, *Transactions American Geophysical Union 89 (33)*, 302–303.

Hu, C., 2009. A novel ocean color index to detect floating algae in the global oceans. *Remote Sensing of Environment 113 (10)*, 2118–2129.

Hu, C., Lee, Z., Ma, R., Yu, K., Li, D., Shang, S., 2010. Moderate resolution imaging spectroradiometer (MODIS) observations of cyanobacteria blooms in Taihu Lake, China. *Journal of Geophysical Research: Oceans (1978–2012) 115 (C4)*, http://doi.org/10.1029/2009JC005511

Kahru, M., Leppänen, J. M., Rud, O., 1993. Cyanobacterial blooms cause heating of the sea surface. *Marine Ecology Progress Series 101*, 1–7.

Kahru, M., 1997. Using satelites to monitor large-scale environmental changes: a case study of cyanobacteri-

al blooms in the Baltic Sea. *Monitoring algal blooms: new techniques for detecting large-scale environmental changes*, Springer-Verlag, Heidelberg Berlin, 43–61.

Kahru, M., Savchuk, O. P., Elmgren, R. (2007). Satellite measurements of cyanobacterial bloom frequency in the Baltic Sea: interannual and spatial variability. *Marine Ecology Progress Series 343*, 15–23.

Kahru, M., Elmgren, R., 2014. Multidecadal time series of satellite-detected accumulations of cyanobacteria in the Baltic Sea. *Biogeosciences 11 (13)*, 3619–3633.

Kaitala, S. 2016. The Alg@line system. Finnish Environment Institute. Source: http://www.finmari-infrastructure.fi/ferrybox. [Accessed on 20.04.2016]

Klapper, H., 1991. *Control of eutrophication in inland waters*. Ellis Horwood Ltd. pp. 1–337.

Kulawiak, M., Lubniewski, Z., 2014. SafeCity—A GIS-based tool profiled for supporting decision making in urban development and infrastructure protection. *Technological Forecasting and Social Change 89*, 174–187, http://doi.org/10.1016/j.techfore.2013.08.031

Kutser, T., 2004. Quantitative detection of chlorophyll in cyanobacterial blooms by satellite remote sensing. *Limnology and Oceanography 49 (6)*, 2179–2189.

Kutser, T., Metsamaa, L., Strömbeck, N., Vahtmäe, E., 2006. Monitoring cyanobacterial blooms by satellite remote sensing. Estuarine, *Coastal and Shelf Science 67 (1)*, 303–312.

Kutser, T., 2009. Passive optical remote sensing of cyanobacteria and other intense phytoplankton blooms in coastal and inland waters. *International Journal of Remote Sensing 30 (17)*, 4401–4425.

Lignell, R., 1993. Effect of vertical cycling on photosynthesis during the annual algal succession in the northern Baltic. *Hydrobiologia 254 (3)*, 159–167.

Mazur-Marzec, H., Browarczyk-Matusiak, G., Forycka, K., Kobos, J., Plinski, M., 2010. Morphological, genetic, chemical and ecophysiological characterisation of two Microcystis aeruginosa isolates from the Vistula Lagoon, southern Baltic. *Oceanologia 52 (1)*, 127–146.

Metsamaa, L., Kutser, T., Strombeck, N., 2006. Recognising cyanobacterial blooms based on their optical signature: a modelling study. *Boreal Environment Research 11 (6)*, 493–506.

Moszynski, M., Kulawiak, M., Chybicki, A., Bruniecki, K., Bielinski, T., Lubniewski, Z., Stepnowski, A., 2015. Innovative Web-based Geographic Information System for Municipal Areas and Coastal Zone Security and Threat Monitoring Using EO Satellite Data. *Marine Geodesy 38 (3)*, 203–224, http://doi.org/10.1080/01490419.2014.969459

Okin, G. S., Gu, J., 2015. The impact of atmospheric conditions and instrument noise on atmospheric correction and spectral mixture analysis of multispectral imagery. *Remote Sensing of Environment 164*, 130–141.

Oyama, Y., Matsushita, B., Fukushima, T., 2014. Distinguishing surface cyanobacterial blooms and aquatic macrophytes using Landsat/TM and ETM+ shortwave infrared bands. *Remote Sensing of Environment 157*, 35–47.

Paldaviciene, A., Mazur-Marzec, H., Razinkovas, A., 2009. Toxic cyanobacteria blooms in the Lithuanian part of the Curonian Lagoon. *Oceanologia 51 (2)*, 203–216.

Pitois, S., Jackson, M. H., Wood, B. J. B., 2000. Problems associated with the presence of cyanobacteria in recreational and drinking waters. International *Journal of Environmental Health Research 10 (3)*, 203–218.

Randolph, K., Wilson, J., Tedesco, L., Li, L., Pascual, D. L., Soyeux, E. (2008). Hyperspectral remote sensing of cyanobacteria in turbid productive water using optically active pigments, chlorophyll a and phycocyanin. *Remote Sensing of Environment 112 (11)*, 4009–4019.

Reinart, A., Kutser, T., 2006. Comparison of different satellite sensors in detecting cyanobacterial bloom events in the Baltic Sea. *Remote Sensing of Environment 102 (1)*, 74–85.

Roy, D. P., Qin, Y., Kovalskyy, V., Vermote, E. F., Ju, J., Egorov, A., Hansen, M. C., Kommareddy, I. Yan, L., 2014. Conterminous United States demonstration and characterization of MODIS-based Landsat ETM+ atmospheric correction. *Remote Sensing of Environment 140*, 433–449.

Rouse, J.W., Jr., Haas, R. H., Deering, D. W., Harlan, J. C. (1974). *Monitoring the vernal advancement and retrogradation (greenwave effect) of natural vegetation*. Texas A & M University, Remote Sensing Center, pp. 1–10.

Ruiz-Verdú, A., Simis, S.G., de Hoyos, C., Gons, H.J., Peña-Martínez, R., 2008. An evaluation of algorithms for the remote sensing of cyanobacterial biomass. Remote Sensing of Environment 112 (11), 3996–4008.

Sivonen, K., Kononen, K., Carmichael, W. W., Dahlem, A. M., Rinehart, K. L., Kiviranta, J., Niemela, S. I., 1989. Occurrence of the hepatotoxic cyanobacterium Nodularia spumigena in the Baltic Sea and structure of the toxin. *Applied and Environmental Microbiology 55 (8)*, 1990–1995.

Sobrino, J.A., Raissouni, N. 2000. Toward remote sensing methods for land cover dynamic monitoring: application to Morocco. *International Journal of Remote Sensing 21 (2)*, 353–366.

SMHI BAWS. 2016. Swedish Meteorological and Hydrological Institute. Source: http://www.smhi.se/en/weather/sweden-weather/1.11631 [Accessed on 20.04.2016]

SYKE Algal Situation service. 2016. Finnish Environment Institute. Source: http://www.environment.fi/algalsituation [Accessed on 20.04.2016]

Stewart, I., Webb, P. M., Schluter, P. J., Fleming, L. E., Burns, J. W., Gantar, M., Backer, L.C. Shaw, G. R., 2006. Epidemiology of recreational exposure to freshwater cyanobacteria–an international prospective cohort study. *BMC Public Health 6 (1)*, http://doi.org/10.1186/1471-2458-6-93

Tanre, D., Holben, B. T., Kaufman, Y. J., 1992. Atmospheric Correction Algorithm for NOAA-AVHRR Products: Theory and Application. *IEEE Transactions on Geoscience and Remote Sensing 30 (2)*, 231–248.

Thell, A.-K., 2013a. Cruise report from KBV001 Poseidon week 9, 2013. Swedish Meteorological and Hydrological Institute. Source: http://www.smhi.se/en/publications/cruise-report-from-kbv001-poseidon-week-9-2013-1.29095 [Accessed on 19.04.2016].

Thell, A.-K., 2013b. Cruise report from KBV001 Poseidon week 25, 2013. Swedish Meteorological and Hydrological Institute. Source: http://www.smhi.se/en/publications/cruise-report-from-kbv-002-triton-week-25-2013-1.31319 [Accessed on 19.04.2016].

Thell, A.-K., 2013c. Cruise report from KBV001 Poseidon week 29, 2013. Swedish Meteorological and Hydrological Institute. Source: http://www.smhi.se/en/publications/cruise-report-from-kbv-002-triton-week-29-2013-1.31898 [Accessed on 19.04.2016].

Thell, A.-K., 2014. Cruise report from R/V Aranda week 28, 2014. Swedish Meteorological and Hydrological Institute. Source: http://www.smhi.se/en/publications/cruise-reports-from-the-marine-monitoring/cruise-report-from-r-v-aranda-week-28-2014-1.77358 [Accessed on 19.04.2016].

Trishchenko, A. P., Hwang, B., Li, Z., 2002. Atmospheric correction of satellite signal in solar domain: impact of improved molecular spectroscopy. *Twelfth ARM Science Team Meeting Proceedings*, St. Petersburg, Florida, 1–7.

USGS AVHRR. 2008. U.S. Geological Survey. Source: http://edc2.usgs.gov/1KM/avhrr_sensor.php [Accessed on 20.04.2016]

Vermote, E. F., El Saleous, N., Roger, J. C., 1995. Operational atmospheric correction of AVHRR visible and near-infrared data. *Atmospheric Sensing and Modelling*, 141–149, http://doi.org/10.1117/12.198596

Vermote, E. F., El Saleous, N. Z., Justice, C. O., 2002. Atmospheric correction of MODIS data in the visible to middle infrared: first results. *Remote Sensing of Environment 83 (1)*, 97–111.

Wang, M., Shi, W., 2007. The NIR-SWIR combined atmospheric correction approach for MODIS ocean color data processing. *Optics Express 15 (24)*, 15722–15733.

Wynne, T. T., Stumpf, R. P., Tomlinson, M. C., Warner, R. A., Tester, P. A., Dyble, J., Fahnenstiel, G. L. (2008). Relating spectral shape to cyanobacterial blooms in the Laurentian Great Lakes. *International Journal of Remote Sensing 29 (12)*, 3665–3672.

Zhao, D., Jiang, H., Yang, T., Cai, Y., Xu, D., An, S., 2012. Remote sensing of aquatic vegetation distribution in Taihu Lake using an improved classification tree with modified thresholds. *Journal of Environmental Management 95 (1)*, 98–107.